Supplemental Material for 'Detection of Spin Entanglement via Spin-Charge Separation in Crossed Tomonaga-Luttinger Liquids'

Alexander Schroer,[1] Bernd Braunecker,[2] Alfredo Levy Yeyati,[3] and Patrik Recher[1,4]

[1] Institut für Mathematische Physik, Technische Universität Braunschweig, D-38106 Braunschweig, Germany
[2] Scottish Universities Physics Alliance, School of Physics and Astronomy, University of St Andrews, North Haugh, St Andrews KY16 9SS, United Kingdom
[3] Departamento de Física Teórica de la Materia Condensada, Condensed Matter Physics Center (IFIMAC), and Instituto Nicolás Cabrera, Universidad Autónoma de Madrid, E-28049 Madrid, Spain
[4] Interactive Research Center of Science, Tokyo Institute of Technology, 2-12-1 Ookayama, Meguro, Tokyo 152-8551, Japan

We give further details about the construction of the generating functional and the nonequilibrium perturbative expansion within the initial state approximation. The direct tunnel contributions to the current and to the current noise are discussed with a special focus on features induced by spin-charge separation. We give the full analytic approximation of the exchange current discussed in the main text and confirm the validity of the initial state approximation and the bias-dependent scaling behavior numerically. The $I(V)$ and $G(V)$ behaviors implied by the scaling behavior are plotted. An alternative implementation using a quantum Hall sample of Corbino geometry is discussed. For brevity we set $a = e = \hbar = v_F = 1$ in intermediate results.

GENERATING FUNCTIONAL AND PERTURBATION THEORY

It is convenient to introduce a contour-ordered generating functional

$$\begin{aligned} Z^{\varphi}_{x_1,x_2} &= \langle\varphi|\, \mathrm{T}_{\mathcal{C}} e^{\int dx \int_{\mathcal{C}} dt \sum_{i\nu s} j_{i\nu s}(x,t)\Phi_{i\nu s}(x,t)}\, |\varphi\rangle \\ &= Z^{\mathrm{dir}}_{x_1,x_2} + \cos(\varphi)\, Z^{\mathrm{exc}}_{x_1,x_2}, \end{aligned} \tag{S1}$$

where $i \in \{1, 2\}$ labels the wire, $\nu \in \{R, L\} \equiv \{1, -1\}$ distinguishes left and right-movers, $s \in \{\uparrow, \downarrow\} \equiv \{1, -1\}$ is the spin index and j a source field. Time-ordering $\mathrm{T}_{\mathcal{C}}$ and the integral in the exponential are performed along the Keldysh contour from t_0 to ∞ (+ branch) and back again ($-$ branch). The relation between the different phase fields reads

$$\Phi_{i\nu s} = \Big(\phi_{i\rho} + s\phi_{i\sigma} + \nu(\theta_{i\rho} + s\theta_{i\sigma})\Big). \tag{S2}$$

We can rewrite the current as

$$I_1 = -\Gamma_{2e} \int dt \sum_{\nu s} \nu \partial_t \frac{\delta Z^{\varphi}_{x_1,x_2}}{\delta j_{1\nu s}(x,t^+)}\Big|_{j=0}, \tag{S3}$$

and the current noise as

$$\begin{aligned} S_{12} = \Gamma_{2e} \mathrm{Re} \int dt d\tilde{t} \sum_{\nu\tilde{\nu}s\tilde{s}} \nu\tilde{\nu}\partial_t\partial_{\tilde{t}} \\ \Big(\frac{\delta^2 Z^{\varphi}_{x_1,x_2}}{\delta j_{1\nu s}(x,t^-)\delta j_{2\tilde{\nu}\tilde{s}}(\tilde{x},\tilde{t}^+)} \\ - \frac{\delta Z^{\varphi}_{x_1,x_2}}{\delta j_{1\nu s}(x,t^-)} \frac{\delta Z^{\varphi}_{x_1,x_2}}{\delta j_{2\tilde{\nu}\tilde{s}}(\tilde{x},\tilde{t}^+)} \Big)\Big|_{j=0}. \end{aligned} \tag{S4}$$

Like any expectation value, the generating functional can be written as a direct and an exchange term. Explicitly, they read in the interaction picture with respect to H_0

$$\begin{aligned} Z^{\mathrm{dir/exc}}_{x_1,x_2} = \frac{1}{4} \sum_{\nu_1\nu_1'\nu_2\nu_2'} \langle \mathrm{T}_{\mathcal{C}} F_{1\nu_1\uparrow} F_{2\nu_2\downarrow} F^{\dagger}_{2\nu_2'\downarrow/\uparrow} F^{\dagger}_{1\nu_1'\uparrow/\downarrow} \\ \exp\Big[\int dx \int_{\mathcal{C}} dt \sum_{i\nu s} j_{i\nu s}(x,t)\Phi_{i\nu s}(x,t) \\ + 2\pi i(\Phi_{1\nu_1\uparrow}(x_1,t_0^-) - \Phi_{1\nu_1'\uparrow/\downarrow}(x_1,t_0^+)) \\ + 2\pi i(\Phi_{2\nu_2\downarrow}(x_2,t_0^-) - \Phi_{2\nu_2'\downarrow/\uparrow}(x_2,t_0^+)) \\ - i\int_{\mathcal{C}} dt\ H_T \Big]\rangle_0 \end{aligned} \tag{S5}$$

with the ground state expectation value $\langle\cdot\rangle_0$ of the unperturbed system. To express all quantities of interest we will use the contour time-ordered correlation functions, following ref. [S1],

$$\begin{aligned} C^{\nu\nu'}_{ss'}(x,t;x',t') &= \langle \mathrm{T}_{\mathcal{C}} \Phi_{i\nu s}(x,t)\Phi_{i\nu' s'}(x',t')\rangle \\ &= -\frac{1}{32\pi^2}\Big((g_\rho^{-1} + \nu + \nu' + \nu\nu' g_\rho)\log(\frac{2\pi}{L} f_{\rho+}) \\ &\quad +(g_\rho^{-1} - \nu - \nu' + \nu\nu' g_\rho)\log(\frac{2\pi}{L} f_{\rho-}) \\ &\quad + ss'(\rho\to\sigma)\Big), \end{aligned} \tag{S6}$$

where

$$f_{\alpha\pm} := -i\mathrm{sgn}_{\mathcal{C}}(t-t')(\pm(x-x') - v_\alpha(t-t')) + a. \tag{S7}$$

The contour sign function $\mathrm{sgn}_{\mathcal{C}}(t - t')$ is 1 whenever t is later on the Keldysh contour than t', and -1 otherwise.

When expanding Z in the tunnel amplitude, the additional Klein factors from the tunnel Hamiltonian impose strong constraints on the internal quantum numbers of the tunnel events. Using the Debye-Waller identity $\langle e^{\sum x_i}\rangle = e^{\frac{1}{2}\langle(\sum x_i)^2\rangle}$ we arrive at

$$
\begin{aligned}
Z^{(0)\mathrm{dir}}_{x_1,x_2} = \frac{1}{4}\sum_{\nu_1\nu_2}\exp\Big[\frac{1}{2}\int dxdx'\int_{\mathcal{C}}dtdt'\sum_{i\nu\nu'ss'}j_{i\nu s}(x,t)j_{i\nu's'}(x',t')C^{\nu\nu'}_{ss'}(x,t;x',t')\\
+2\pi i\int dx\int_{\mathcal{C}}dt\sum_{\nu s}\Big[j_{1\nu s}(x,t)\Big(C^{\nu\nu_1}_{s\uparrow}(x,t;x_1,t_0^-)-C^{\nu\nu_1}_{s\uparrow}(x,t;x_1,t_0^+)\Big)\\
+j_{2\nu s}(x,t)\Big(C^{\nu\nu_2}_{s\downarrow}(x,t;x_2,t_0^-)-C^{\nu\nu_2}_{s\downarrow}(x,t;x_2,t_0^+)\Big)\Big]\Big],
\end{aligned}
\tag{S8}
$$

$$
\begin{aligned}
Z^{(2)\mathrm{dir}}_{x_1,x_2} = -|T|^2\int_{\mathcal{C}}dt'dt''\sum_{\nu_1\nu_2}\exp\Big[\frac{1}{2}\int dxdx'\int_{\mathcal{C}}dtdt'\sum_{i\nu\nu'ss'}j_{i\nu s}(x,t)j_{i\nu's'}(x',t')C^{\nu\nu'}_{ss'}(x,t;x',t')\Big]\\
\times\Big[\sum_{\nu'\nu''s'}\exp\Big[+2\pi i\int dx\int_{\mathcal{C}}dt\sum_{\nu s}\Big[j_{1\nu s}(x,t)\Big(C^{\nu\nu_1}_{s\uparrow}(x,t;x_1,t_0^-)-C^{\nu\nu_1}_{s\uparrow}(x,t;x_1,t_0^+)\\
+C^{\nu\nu'}_{ss'}(x,t;0,t')-C^{\nu\nu'}_{ss'}(x,t;0,t'')\Big)\\
+j_{2\nu s}(x,t)\Big(C^{\nu\nu_2}_{s\downarrow}(x,t;x_2,t_0^-)-C^{\nu\nu_2}_{s\downarrow}(x,t;x_2,t_0^+)\\
-C^{\nu\nu''}_{ss'}(x,t;0,t')+C^{\nu\nu''}_{ss'}(x,t;0,t'')\Big)\Big]\Big]\\
\times\langle\nu_1\uparrow,\nu_2\downarrow|\,\mathrm{T}_{\mathcal{C}}\mathcal{H}^{Ts'}_{1\nu'\to2\nu''}(t')\mathcal{H}^{Ts'}_{2\nu''\to1\nu'}(t'')\,|\nu_1\uparrow,\nu_2\downarrow\rangle\\
+\sum_{\nu'}\exp\Big[+2\pi i\int dx\int_{\mathcal{C}}dt\sum_{\nu s}\Big[j_{1\nu s}(x,t)\Big(C^{\nu\nu_1}_{s\uparrow}(x,t;x_1,t_0^-)-C^{\nu,-\nu_1}_{s\uparrow}(x,t;x_1,t_0^+)\\
+C^{\nu,-\nu_1}_{ss'}(x,t;0,t')-C^{\nu,-\nu_1}_{ss'}(x,t;0,t'')\Big)\\
+j_{2\nu s}(x,t)\Big(C^{\nu\nu_2}_{s\downarrow}(x,t;x_2,t_0^-)-C^{\nu\nu_2}_{s\downarrow}(x,t;x_2,t_0^+)\\
-C^{\nu\nu'}_{ss'}(x,t;0,t')+C^{\nu\nu'}_{ss'}(x,t;0,t'')\Big)\Big]\Big]\\
\times\langle\nu_1\uparrow,\nu_2\downarrow|\,\mathrm{T}_{\mathcal{C}}\mathcal{H}^{Ts'}_{1,-\nu_1\to2\nu'}(t')\mathcal{H}^{Ts'}_{2\nu'\to1\nu_1}(t'')\,|-\nu_1\uparrow,\nu_2\downarrow\rangle\\
+\sum_{\nu'}\exp\Big[+2\pi i\int dx\int_{\mathcal{C}}dt\sum_{\nu s}\Big[j_{1\nu s}(x,t)\Big(C^{\nu\nu_1}_{s\uparrow}(x,t;x_1,t_0^-)-C^{\nu\nu_1}_{s\uparrow}(x,t;x_1,t_0^+)\\
+C^{\nu\nu'}_{ss'}(x,t;0,t')-C^{\nu\nu'}_{ss'}(x,t;0,t'')\Big)\\
+j_{2\nu s}(x,t)\Big(C^{\nu\nu_2}_{s\downarrow}(x,t;x_2,t_0^-)-C^{\nu,-\nu_2}_{s\downarrow}(x,t;x_2,t_0^+)\\
-C^{\nu\nu_2}_{ss'}(x,t;0,t')+C^{\nu,-\nu_2}_{ss'}(x,t;0,t'')\Big)\Big]\Big]\\
\times\langle\nu_1\uparrow,\nu_2\downarrow|\,\mathrm{T}_{\mathcal{C}}\mathcal{H}^{Ts'}_{1\nu'\to2\nu_2}(t')\mathcal{H}^{Ts'}_{2,-\nu_2\to1\nu'}(t'')\,|\nu_1\uparrow,-\nu_2\downarrow\rangle\Big]
\end{aligned}
\tag{S9}
$$

and

$$
\begin{aligned}
Z^{(2)\mathrm{exc}}_{x_1,x_2} = -|T|^2\int_{\mathcal{C}}dt'dt''\sum_{\nu_1\nu_1'\nu_2\nu_2'}\exp\Big[\frac{1}{2}\int dxdx'\int_{\mathcal{C}}dtdt'\sum_{i\nu\nu'ss'}j_{i\nu s}(x,t)j_{i\nu's'}(x',t')C^{\nu\nu'}_{ss'}(x,t;x',t')\\
+2\pi i\int dx\int_{\mathcal{C}}dt\sum_{\nu s}\Big[j_{1\nu s}(x,t)\Big(C^{\nu\nu_1}_{s\uparrow}(x,t;x_1,t_0^-)-C^{\nu\nu_1'}_{s\downarrow}(x,t;x_1,t_0^+)\\
+C^{\nu\nu_1'}_{s\downarrow}(x,t;0,t')-C^{\nu\nu_1}_{s\uparrow}(x,t;0,t'')\Big)\\
+j_{2\nu s}(x,t)\Big(C^{\nu\nu_2}_{s\downarrow}(x,t;x_2,t_0^-)-C^{\nu\nu_2'}_{s\uparrow}(x,t;x_2,t_0^+)\\
-C^{\nu\nu_2}_{s\downarrow}(x,t;0,t')+C^{\nu\nu_2'}_{s\uparrow}(x,t;0,t'')\Big)\Big]\Big]\\
\times\langle\nu_1\uparrow,\nu_2\downarrow|\,\mathrm{T}_{\mathcal{C}}\mathcal{H}^{T\downarrow}_{1\nu_1'\to2\nu_2}(t')\mathcal{H}^{T\uparrow}_{2\nu_2'\to1\nu_1}(t'')\,|\nu_1'\downarrow,\nu_2'\uparrow\rangle\,,
\end{aligned}
\tag{S10}
$$

where we have decomposed the tunnel Hamiltonian $H_T = T\sum_{i\nu\nu' s}\mathcal{H}^{Ts}_{i\nu\to\bar{i}\nu'}$ into the processes in which a ν-moving spin-s electron tunnels from wire i into wire $\bar{i}$, becoming a ν'-mover. The relevant amplitudes are

$$\begin{aligned}\langle \nu_1\uparrow,\nu_2\downarrow|\mathrm{T}_\mathcal{C}\mathcal{H}^{Ts}_{1\nu\to 2\nu'}(t')\mathcal{H}^{Ts}_{2\nu'\to 1\nu}(t'')\,|\nu_1\uparrow,\nu_2\downarrow\rangle &= \frac{a^{(g^{-1}+g-2)/2}}{4(2\pi)^2}\Big[f_\rho^{-\frac{g^{-1}+g}{2}}f_\sigma^{-1}\Big](0,t';0,t'')\\ &\times \Xi_{\nu_1\nu s}(x_1,t_0^-;0,t')\Xi_{\nu_1\nu s}(x_1,t_0^+;0,t'')\Xi^{-1}_{\nu_1\nu s}(x_1,t_0^-;0,t'')\Xi^{-1}_{\nu_1\nu s}(x_1,t_0^+;0,t')\\ &\times \Xi^{-1}_{\nu_2\nu'\,-s}(x_2,t_0^-;0,t')\Xi_{\nu_2\nu'\,-s}(x_2,t_0^-;0,t'')\Xi_{\nu_2\nu'\,-s}(x_2,t_0^+;0,t')\Xi^{-1}_{\nu_2\nu'\,-s}(x_2,t_0^+;0,t'')\end{aligned}\tag{S11}$$

and

$$\begin{aligned}\langle R\uparrow,R\downarrow|\mathrm{T}_\mathcal{C}\mathcal{H}^{T\downarrow}_{1R\to 2R}(t')\mathcal{H}^{T\uparrow}_{2R\to 1R}(t'')\,|R\downarrow,R\uparrow\rangle &= -\frac{a^{(g^{-1}+g+2)/2}}{4(2\pi)^2}\Big[f_\rho^{-\frac{g^{-1}+g}{2}}f_\sigma\Big](0,t';0,t'')\\ &\times \Xi_{RR\downarrow}(x_1,t_0^-;0,t')\Xi_{RR\downarrow}(x_1,t_0^+;0,t'')\Xi_{RR\downarrow}(x_2,t_0^-;0,t'')\Xi_{RR\downarrow}(x_2,t_0^+;0,t')\\ &\times \Xi^{-1}_{RR\uparrow}(x_1,t_0^-;0,t'')\Xi^{-1}_{RR\uparrow}(x_1,t_0^+;0,t')\Xi^{-1}_{RR\uparrow}(x_2,t_0^-;0,t')\Xi^{-1}_{RR\uparrow}(x_2,t_0^+;0,t'')\end{aligned}\tag{S12}$$

with the abbreviation

$$\Xi_{\nu\nu' s} = f_{\rho+}^{\frac{g^{-1}+\nu+\nu'+\nu\nu' g}{8}}f_{\rho-}^{\frac{g^{-1}-\nu-\nu'+\nu\nu' g}{8}}f_{\sigma\nu}^{\frac{1+\nu\nu'}{4s}}. \tag{S13}$$

Substituting this into Eqs. (S3) and (S4), the functional derivatives and the t and $\tilde{t}$-integral can be performed in a straightforward fashion. For the integration we use that $x,\tilde{x}\gg a$. The result is independent of the measurement points x and $\tilde{x}$ and the measurement times t and $\tilde{t}$, because, irrespective of when the electrons are injected and of how far they have to travel before being measured, they will be detected eventually. More importantly, in the second order corrections only terms for which the tunneling times t' and t'' lie on different branches of the Keldysh contour survive. Identifying the integral over the first order tunnel Hamiltonian with the interaction picture time evolution operator, $-iT\int_{t_0}^\infty dt\mathcal{H}^{Ts}_{i\nu\to\bar{i}\nu'} =: U^{(1)s}_{i\nu\to\bar{i}\nu'}$, this leads to the expressions given in the main text, where all $2k_F$-processes have been dropped. This is a good approximation (which has been checked numerically), because they always require at least one initial left-mover to tunnel. In the presence of interactions injected left-movers decay into a large left- and a small right-moving charge excitation (charge fractionalisation) and the spin excitation moves completely to the left, because there are no interactions in the spin sector. In the particular geometry under consideration, where the injection point is on the left of the tunnel junction, this means that the tunneling of initial left-movers is strongly suppressed, because most of the excitation does not reach the junction. In the spin sector this is still valid for a beam splitter adiabatically coupled to Fermi liquid leads described by a $g(x)$ model [S2–S4], whereas for the charge excitations additional reflections at the boundary to the Fermi liquid leads would appear. However, for generic length of the wires, we do not expect qualitative changes of the result.

DIRECT CONTRIBUTIONS

The direct tunneling corrections of the current and of the current noise are

$$\begin{aligned}I_1{}^{(2)\mathrm{dir}} &= -e\Gamma_{2e}\sum_{\nu_1\nu_2\nu\nu' s}\frac{1+\nu g}{2}\\ &\times\Big[||U^{(1)s}_{2\nu'\to 1\nu}\,|\nu_1\uparrow,\nu_2\downarrow\rangle\,||^2 - ||U^{(1)s}_{1\nu\to 2\nu'}\,|\nu_1\uparrow,\nu_2\downarrow\rangle\,||^2\Big],\end{aligned}\tag{S14}$$

$$\begin{aligned}S_{12}{}^{(2)\mathrm{dir}} &= -e^2\Gamma_{2e}\sum_{\nu_1\nu_2\nu\nu' s}\frac{1+\nu g}{2}\frac{1+\nu' g}{2}\\ &\times\mathrm{Re}\Big[||U^{(1)s}_{2\nu'\to 1\nu}\,|\nu_1\uparrow,\nu_2\downarrow\rangle\,||^2 + ||U^{(1)s}_{1\nu\to 2\nu'}\,|\nu_1\uparrow,\nu_2\downarrow\rangle\,||^2\Big].\end{aligned}\tag{S15}$$

We notice that the magnitude of these expressions is set by the standard quantum mechanical probability of the final state $||\cdot||^2$. This is in contrast to the exchange processes discussed in the main text, in which the magnitude is given by spin-flipped amplitudes, underlining the role of the exchange contribution as a nonclassical interference effect. Note that U only includes the part of the tunnel Hamiltonian denoted by its indices and is, therefore, not unitary.

The direct contributions are mostly constant, but they show additional features for certain injection points $x_{1,2}$ (Fig. S1a,c).

The tunnel correction is always negative, because all tunnel events $1\to 2$ decrease the current after the junction, whereas $2\to 1$ increase it only if the electron becomes a right mover. The correction is weaker at higher interaction strength (smaller g), which is related to the well-known suppression of the tunnel density of states in Tomonaga-Luttinger liquids (TLL) [S5] and can be traced back to that fact that electrons are no eigenmodes of the theory.

In contrast to the exchange current, increasing the distance between the injection point and the tunnel junction does not suppress the direct current, because spin

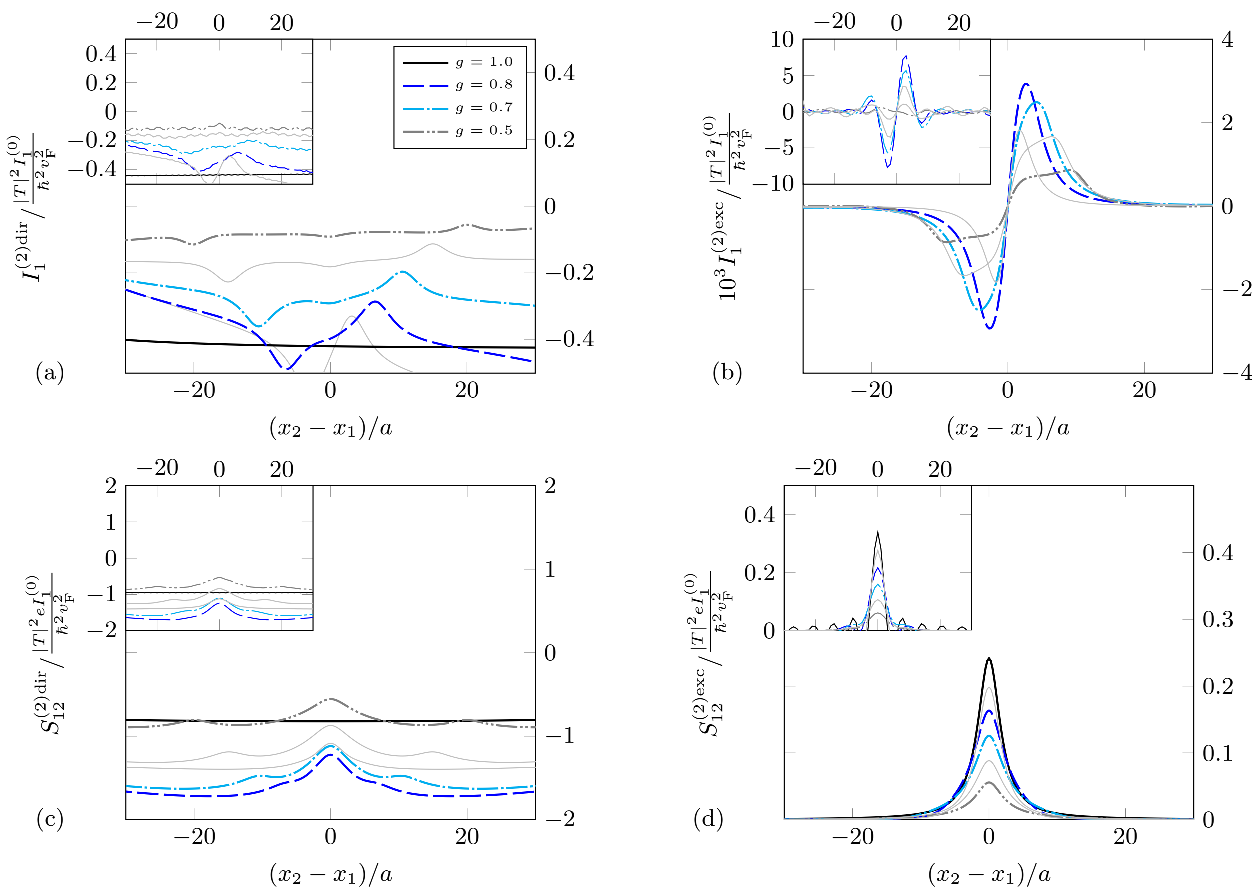

FIG. S1. (a) direct and (b) exchange current, (c) direct and (d) exchange current noise. Insets: a large voltage bias modeled as an injection Hamiltonian with a Peierls phase reproduces the initial state approximation for large voltages $2eV \to \hbar v_F a^{-1}$ up to residual oscillations.

compensation is not required. As discussed in the main text, a charge (spin) imbalance across the junction gives rise to a charge (spin) average current. As a consequence there is a tunnel current even if the injected electron has completely disintegrated into spatially separated charge and spin modes by the time it reaches the junction. This holds even though the electron propagator $\langle \Psi_\sigma(x,t)\Psi_\sigma^\dagger(0,0)\rangle$ is algebraically suppressed in space x and time t (precisely due to spin-charge separation), because a Wick decomposition is not allowed in this interacting system.

Similar to the exchange current, there is a two-particle correlation effect: tunneling of charge excitations is suppressed if a charge or a spin excitation arrives simultaneously at the tunnel junction in the other wire. Two charge excitations can meet only if $x_1 = x_2$. In this case, both the in- and out-tunneling rates are reduced and so the total effect is very small. However, only charge out-tunneling is reduced if the charge excitation of electron 1 arrives simultaneously with the spin excitation of electron 2, i.e., $x_1/v_\rho = x_2/v_\sigma$. Conversely, charge in-tunneling is reduced if the charge excitation of electron 2 meets the spin excitation of electron 1 at the junction, i.e., $x_1/v_\sigma = x_2/v_\rho$. This produces secondary features, which are a signature of spin-charge separation (cf. Fig. S1a,c).

The current noise shows the same behavior, except that it is always reduced, irrespective of whether in- or out-tunneling is suppressed. This changes the sign of half the features, but leaves their position unchanged (Fig. S1c). The noise is negative, because due to charge conservation δI_1 and δI_2 have opposite signs in all processes.

Similar side dips have recently been found theoretically in the noise of collective excitations in chiral edge channels [S6].

ANALYTIC APPROXIMATION

The spin-flipped overlap integral $P_{1\to 2}$ used in the analytic approximation of the exchange current reads

$$\begin{aligned} P_{1\to 2} &:= \sum_{t',t''} \langle \psi_{1R\uparrow}(x_1,t_0)\psi^\dagger_{1R\uparrow}(0,t'')\psi_{1R\downarrow}(0,t')\psi^\dagger_{1R\downarrow}(x_1,t_0)\rangle_1 \langle \psi_{2R\downarrow}(x_2,t_0)\psi_{2R\uparrow}(0,t'')\psi^\dagger_{2R\downarrow}(0,t')\psi^\dagger_{2R\uparrow}(x_2,t_0)\rangle_2 \\ &\propto \sum_{t',t''} \langle R\uparrow, R\downarrow|\, \mathrm{T}_{\mathcal{C}} \mathcal{H}^{T\downarrow}_{1R\to 2R}(t'^{+})\mathcal{H}^{T\uparrow}_{2R\to 1R}(t''^{-})\,|R\downarrow, R\uparrow\rangle\,. \end{aligned} \tag{S16}$$

Starting from Eq. (S12), this can be written as

$$\begin{aligned} P_{1\to 2} \propto \sum_{t',t''} &\Big(\frac{i}{g}(t'-t'')+1\Big)^{-\frac{g^{-1}+g}{2}} \Big(i(t'-t'')+1\Big) \\ &\times \Big((x_1+t')^2+1\Big)^{-\frac{1}{2}} \Big((x_1+t'')^2+1\Big)^{-\frac{1}{2}} \Big((x_2+t')^2+1\Big)^{-\frac{1}{2}} \Big((x_2+t'')^2+1\Big)^{-\frac{1}{2}} \\ &\times \exp\Big[i\frac{g^{-1}+g+2}{4}\Big(\arctan(x_1+t'/g)-\arctan(x_1+t''/g)-\arctan(x_2+t'/g)+\arctan(x_2+t''/g)\Big) \\ &\qquad + i\frac{g^{-1}+g-2}{4}\Big(\arctan(-x_1+t'/g)-\arctan(-x_1+t''/g)-\arctan(-x_2+t'/g)+\arctan(-x_2+t''/g)\Big)\Big], \end{aligned} \tag{S17}$$

where we chose $t_0 = 0$. To extract the behavior at large injection distances, it suffices to consider absolute values and charge fractionalization can be dropped, because it is inessential for the spin exchange. So we discard the exponential factor, approximate $g^{-1}+g+2 \approx 4$ and perform a standard Taylor series expansion around $(x_1+x_2)^{-1} = 0$.

BIASED INJECTION

Instead of relying on the initial state approximation, the injection can be modeled by a second tunnel Hamiltonian which takes into account the voltage induced phase difference as a Peierls phase [S7]:

$$\begin{aligned} H_I(t) &= Ie^{i\frac{2eV}{\hbar}t}\sum_{\nu_1\nu_2}\Big[\psi_{1\nu_1\uparrow}(x_1,t)\psi_{2\nu_2\downarrow}(x_2,t) \\ &\qquad\qquad + e^{i\varphi}\psi_{1\nu_1\downarrow}(x_1,t)\psi_{2\nu_2\uparrow}(x_2,t)\Big] + \text{h.c.} \\ &= I\sum_{\nu_1\nu_2\zeta}\Big(\mathcal{H}^{I\mathrm{dir}(\zeta)}_{\nu_1\nu_2} + e^{i\varphi}\mathcal{H}^{I\mathrm{exc}(\zeta)}_{\nu_1\nu_2}\Big). \end{aligned} \tag{S18}$$

For sufficiently low injection rates there are no correlations between subsequently injected pairs and we can restrict the perturbative expansion to leading, i.e., second order in the injection amplitude I. Due to particle number conservation, tunneling and injection each enter at even orders only. All terms which are of zeroth order in the injection are equilibrium contributions and do not carry a current or cross-wire noise. The new generating functional is of the form

$$Z = Z^{(2I)} + Z^{(2I,2T)} + \dots, \tag{S19}$$

where the superscripts denote the expansion order in injection I and tunneling T. All expectation values are then taken with respect to the ground state. Special care has to be taken when contracting the Klein factors. Although not explicitly time dependent they need to be time-ordered which can introduce signs. The no-tunneling contributions are

$$I_1^{(2I)} = -\frac{ev_F}{a}\Big|\frac{I}{\hbar v_F}\Big|^2 \frac{\pi 2^{4\gamma}}{\Gamma(4\gamma)}\mathrm{sgn}(V)\Big|\frac{ea}{\hbar v_F}V\Big|^{4\gamma-1}, \tag{S20}$$

and

$$S_{12}^{(2I)} = \frac{e}{2}|I_1^{(2I)}|, \tag{S21}$$

where $\gamma = \frac{g^{-1}+g+2}{8}$. The current shows a characteristic power law behavior which is expected since it applies to any TLL point injection calculation [S3, S8]. Likewise, the finite noise contribution is shot noise generated in the injection process. Note that the Schottky-like cross-correlation S_{12} does not contain an anomalous charge, which has been reported for the auto-correlation of infinite TLLs [S8].

The leading order contributions are

$$I_1^{(2I,2T)\mathrm{dir}} = -|I|^2|T|^2 \sum_{\lambda_i\nu_1\nu_2\nu\nu' s} \lambda_0\lambda_1\lambda_2\lambda_3\Big(\frac{1+g}{2}(\lambda_0-\lambda_1)+\frac{1+\nu g}{2}(\lambda_2-\lambda_3)\Big)$$
$$\times \int\Big(\prod_{m=1\dots 3} d\tau_m\Big)\left\langle \mathrm{T}_{\mathcal{C}}\mathcal{H}^{I\mathrm{dir}}_{\nu_1\nu_2}(0^{\lambda_0})\mathcal{H}^{I\mathrm{dir}\dagger}_{\nu_1\nu_2}(\tau_1^{\lambda_1})\mathcal{H}^{Ts}_{1\to 2,\nu\to\nu'}(\tau_2^{\lambda_2})\mathcal{H}^{Ts}_{2\to 1,\nu'\to\nu}(\tau_3^{\lambda_3})\right\rangle, \quad \text{(S22)}$$

$$I_1^{(2I,2T)\mathrm{exc}} = -|I|^2|T|^2\frac{1+g}{2} \sum_{\lambda_i} \lambda_0\lambda_1\lambda_2\lambda_3\Big((\lambda_0-\lambda_1)+(\lambda_2-\lambda_3)\Big)$$
$$\times \int\Big(\prod_{m=1\dots 3} d\tau_m\Big)\left\langle \mathrm{T}_{\mathcal{C}}\mathcal{H}^{I\mathrm{dir}}_{RR}(0^{\lambda_0})\mathcal{H}^{I\mathrm{exc}\dagger}_{RR}(\tau_1^{\lambda_1})\mathcal{H}^{T\downarrow}_{1\to 2,R\to R}(\tau_2^{\lambda_2})\mathcal{H}^{T\uparrow}_{2\to 1,R\to R}(\tau_3^{\lambda_3})\right\rangle, \quad \text{(S23)}$$

$$S_{12}^{(2I,2T)\mathrm{dir}} = \frac{|I|^2|T|^2}{2} \sum_{\substack{\lambda_i\nu_1\nu_2\\ \nu\nu' s}} \lambda_0\lambda_1\lambda_2\lambda_3\Big[\Big((\lambda_0-\lambda_1)\frac{1+g}{2}+(\lambda_2-\lambda_3)\frac{1+\nu g}{2}\Big)\Big((\lambda_0-\lambda_1)\frac{1+g}{2}-(\lambda_2-\lambda_3)\frac{1+\nu' g}{2}\Big)\Big]$$
$$\times \int\Big(\prod_{m=1\dots 3} d\tau_m\Big)\left\langle \mathrm{T}_{\mathcal{C}}\mathcal{H}^{I\mathrm{dir}}_{\nu_1\nu_2}(0^{\lambda_0})\mathcal{H}^{I\mathrm{dir}\dagger}_{\nu_1\nu_2}(\tau_1^{\lambda_1})\mathcal{H}^{Ts}_{1\to 2,\nu\to\nu'}(\tau_2^{\lambda_2})\mathcal{H}^{Ts}_{2\to 1,\nu'\to\nu}(\tau_3^{\lambda_3})\right\rangle, \quad \text{(S24)}$$

$$S_{12}^{(2I,2T)\mathrm{exc}} = \frac{|I|^2|T|^2}{2}\Big(\frac{1+g}{2}\Big)^2 \sum_{\lambda_i} \lambda_0\lambda_1\lambda_2\lambda_3\Big[\Big((\lambda_0-\lambda_1)+(\lambda_2-\lambda_3)\Big)\Big((\lambda_0-\lambda_1)-(\lambda_2-\lambda_3)\Big)\Big]$$
$$\times \int\Big(\prod_{m=1\dots 3} d\tau_m\Big)\left\langle \mathrm{T}_{\mathcal{C}}\mathcal{H}^{I\mathrm{dir}}_{RR}(0^{\lambda_0}))\mathcal{H}^{I\mathrm{exc}\dagger}_{RR}(\tau_1^{\lambda_1})\mathcal{H}^{T\downarrow}_{1\to 2,R\to R}(\tau_2^{\lambda_2})\mathcal{H}^{T\uparrow}_{2\to 1,R\to R}(\tau_3^{\lambda_3})\right\rangle, \quad \text{(S25)}$$

where $\lambda_i = \pm 1$ indicates which part of the Keldysh contour the time τ^{λ_i} lies on. At large voltages, a numeric integration reproduces the results of the initial state approximation (Fig. S1, insets). The overlap integrals $\mathcal{I} = \int d\tau\langle\cdots\rangle$ are of the general form

$$\mathcal{I}(\{x\},V,a) = \frac{1}{a^{\alpha+2}}\int\Big(\prod_{m=1\dots 3} d\tau_m\Big)e^{2iV\tau_1}\prod_n\Big(i(x_n\pm v_n\tau_n)+a\Big)^{\alpha_n}, \quad \text{(S26)}$$

up to constant prefactors, where $\alpha=\sum_n\alpha_n$. With η a number we then derive the exact scaling law

$$\begin{aligned}
\mathcal{I}(\{x\},\eta V,a) &= \frac{1}{a^{\alpha+2}}\int\Big(\prod_{m=1\dots 3} d\tau_m\Big)e^{2i\eta V\tau_1}\prod_n\Big(i(x_n\pm v_n\tau_n)+a\Big)^{\alpha_n}\\
&= \frac{\eta^{-1}}{(\eta a)^{\alpha+2}}\int\Big(\prod_{m=1\dots 3} d\tilde\tau_m\Big)e^{2iV\tilde\tau_1}\prod_n\Big(i(\eta x_n\pm v_n\tilde\tau_n)+\eta a\Big)^{\alpha_n}\\
&= \eta^{-1}\mathcal{I}(\{\eta x\},V,\eta a), \qquad \text{(S27)}
\end{aligned}$$

where we have substituted $\tilde\tau=\eta\tau$. Assuming that the integral is independent of the high energy cutoff at low voltages and/or large injection distances, an approximate scaling law can be obtained by neglecting the scaling of a against that of $i(x-v\tau)$:

$$\begin{aligned}
\mathcal{I}(\{x\},\eta V,a) &= \frac{\eta^{-1}}{(\eta a)^{\alpha+2}}\int\Big(\prod_{m=1\dots 3} d\tilde\tau_m\Big)e^{2iV\tilde\tau_1}\prod_n\Big(i(\eta x_n\pm v_n\tilde\tau_n)+\eta a\Big)^{\alpha_n}\\
&\approx \frac{\eta^{-1}}{(\eta a)^{\alpha+2}}\int\Big(\prod_{m=1\dots 3} d\tilde\tau_m\Big)e^{2iV\tilde\tau_1}\prod_n\Big(i(\eta x_n\pm v_n\tilde\tau_n)+a\Big)^{\alpha_n}\\
&= \eta^{-3-\alpha}\mathcal{I}(\{\eta x\},V,a). \qquad \text{(S28)}
\end{aligned}$$

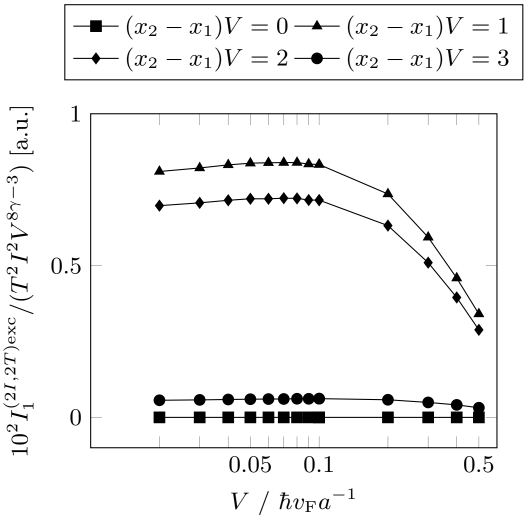

FIG. S2. When lowering the voltage and simultaneously rescaling x_1 and x_2, the exchange current follows a power law. At large bias voltages, $eV \gtrsim 0.1\hbar v_F a^{-1}$, the influence of the high energy cutoff is still visible. The parameters are $g = 0.8$ and $(x_1 + x_2)V = -15a$.

The validity of this approximation has been confirmed numerically (Fig. S2). Specifying α leads to the scaling behavior given in the main text.

The scaling law implies that lowering the injection voltage corresponds to increasing all length scales, so the current-voltage relation $I(V)$ (Fig. S3a) and the conductance-voltage relation $G(V)$ (Fig. S3b) pick up the nonmonotonous behavior of the exchange current already present in Fig. 2. Therefore, it is not necessary in an experiment to actually change the injection points $x_{1,2}$.

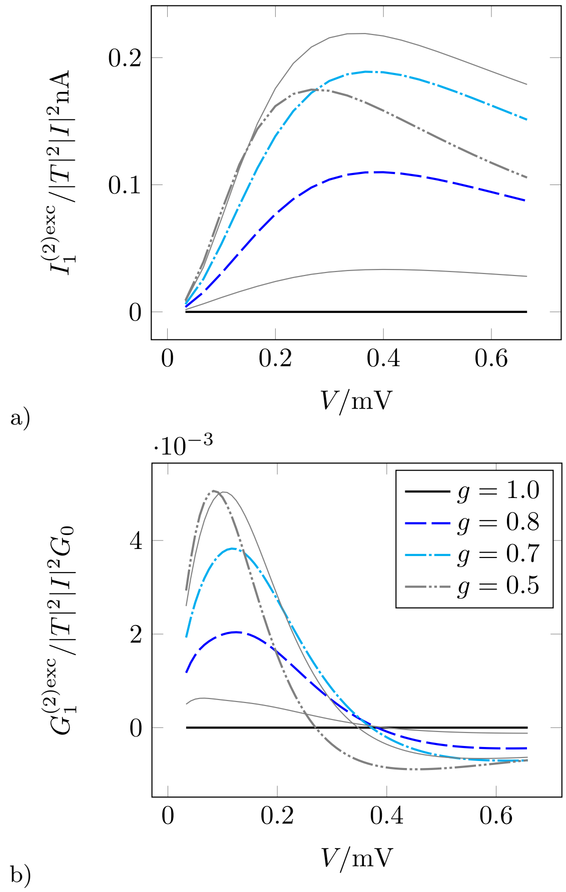

FIG. S3. a) Exchange current in wire 1 according to scaling relation (12) for different injection voltages and interaction parameters g within an experimentally realistic range. The injection points are fixed at $x_1 = 1500$ nm, $x_2 = 900$ nm. Gray lines represent equidistant intermediate g values. The material parameters are the same as in the main text. Note the nonmonotonous behavior similar to Fig. 2 in the main text. b) The corresponding conductance.

QUANTUM HALL DEVICE

Beam splitters have been successfully implemented as integer quantum Hall (QH) devices [S9–S12]. Cooper pair splitters are likely to suffer from the strong magnetic field, but recently a new correlated pair source for QH edge states has been realized [S13], which may allow for the injection of spin-entangled electrons. Concerning the beam splitter itself, a QH device offers considerable advantages. Being chiral, the edge state of the QH effect have a very large mean free path and a coherence length up to several 10 μm. Chirality also implies the absence of charge fractionalization, which is an unwanted effect in our device. The intended geometry can be fabricated with high precision and fine tuned via appropriate gating in a running experiment thus giving immediate access to the injection distances $|x_{1,2}|$. Therefore we will explain how the results for the nanowires have to be modified in this section.

The beam splitter can be realized as a constriction in a ring-shaped Corbino QH sample (Fig. S4). The sample has to be operated at a Zeeman splitting much smaller than the Landau splitting, such that at each edge two copropagating channels of opposite spin form. Due to the difference in Zeeman energy, at a fixed Fermi energy opposite spins have different Fermi vectors and are slightly separated in real space. This has already been demonstrated experimentally [S14]. When linearizing the spectrum around the Fermi points, where we assume the Fermi velocity v_F to be independent of edge and spin, the electrostatic repulsion between and within the channels can be treated exactly using bosonization. This yields two spinful chiral TLLs,

$$H_0 = \sum_{i\alpha} \int dx \hbar v_\alpha \Big(\frac{\partial \phi_{i\alpha}}{\partial x}\Big)^2, \tag{S29}$$

where $\alpha \in \{\rho, \sigma\}$ labels the charge and the spin channel at edge $i \in \{1, 2\}$. As in the nanowire, the charge veloc-

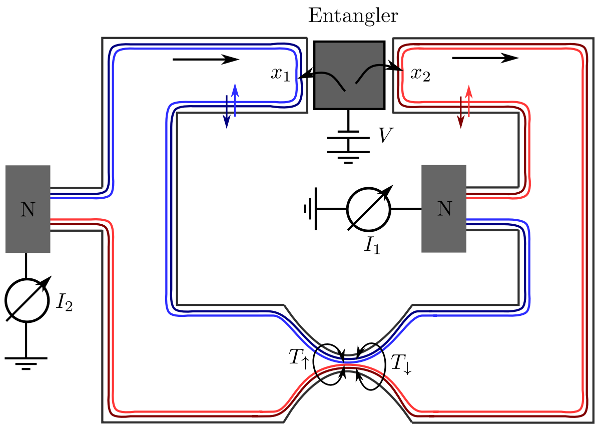

FIG. S4. Beam splitter realized in a quantum Hall sample of Corbino geometry. Two copropagating channels with opposite spin form a spinful chiral TLL at each edge. At a finite Zeeman splitting, they are spatially separated and the tunnel amplitudes at the constriction become spin dependent.

ity exceeds the spin velocity, $v_\rho > v_\sigma = v_F$. The electron field is $\psi_{js}(x) = (2\pi a)^{-1/2} F_{js} \exp\Big[ik_s x + 2\pi i \Phi_{js}(x)\Big]$ where $\Phi_{js} = \sqrt{\pi/2}(\phi_{j\rho} + s\phi_{j\sigma})$ with $s \in \{\uparrow,\downarrow\}$ the spin index and k_s the spin-dependent Fermi vector. The tunnel Hamiltonian becomes

$$\begin{aligned} H_T &= \sum_s \Big(T_s \psi_{1s}^\dagger(0)\psi_{2s}(0) + T_s^\star \psi_{2s}^\dagger(0)\psi_{1s}(0)\Big) \\ &= \sum_s \Big(T_s \mathcal{H}^{Ts}_{2\to 1} + T_s^\star \mathcal{H}^{Ts}_{1\to 2}\Big), \end{aligned} \tag{S30}$$

where the tunnel amplitude T_s is in general complex because of the magnetic field and spin dependent, because at the constriction tunneling happens between the outer and the inner channels respectively (cf. Fig. S4). TLL behavior has already been investigated and observed in this system [S6, S15].

The initial state is

$$\begin{aligned} |\varphi\rangle &= \sqrt{2}\pi a \Big(\psi^\dagger_{2\downarrow}(x_2)\psi^\dagger_{1\uparrow}(x_1) + e^{i\varphi}\psi^\dagger_{2\uparrow}(x_2)\psi^\dagger_{1\downarrow}(x_1)\Big) |\rangle \\ &:= 2^{-1/2}(|\uparrow,\downarrow\rangle + e^{i\varphi}|\downarrow,\uparrow\rangle). \end{aligned} \tag{S31}$$

Lacking SU(2) spin invariance, the direct and exchange contributions have to be redefined as $\frac{1}{2}(\langle\uparrow,\downarrow|\,\mathcal{O}\,|\uparrow,\downarrow\rangle + \langle\downarrow,\uparrow|\,\mathcal{O}\,|\downarrow,\uparrow\rangle)$ and $\frac{1}{2}(e^{i\varphi}\langle\uparrow,\downarrow|\,\mathcal{O}\,|\downarrow,\uparrow\rangle + e^{-i\varphi}\langle\downarrow,\uparrow|\,\mathcal{O}\,|\uparrow,\downarrow\rangle)$.

The calculation proceeds in analogy to the nanowire model and without further approximations one finds

$$\begin{aligned} I_1^{(2)\mathrm{dir}} =& - e\Gamma_{2e}\frac{|T_\uparrow|^2 + |T_\downarrow|^2}{\hbar^2 v_F^2} \\ &\times \sum_s \Big[||U^{(1)s}_{2\to 1}|\uparrow,\downarrow\rangle||^2 - ||U^{(1)s}_{1\to 2}|\uparrow,\downarrow\rangle||^2\Big], \end{aligned} \tag{S32}$$

$$\begin{aligned} I_1^{(2)\mathrm{exc}} =& \, e\Gamma_{2e}\frac{\mathrm{Re}(T_\uparrow^\star T_\downarrow e^{i(k_\uparrow - k_\downarrow)(x_1-x_2)+i\varphi})}{\hbar^2 v_F^2} \\ &\times \Big[\langle\uparrow,\downarrow|\, U^{(1)\uparrow\dagger}_{1\to 2} U^{(1)\downarrow}_{1\to 2}|\downarrow,\uparrow\rangle - \langle\uparrow,\downarrow|\, U^{(1)\downarrow\dagger}_{2\to 1} U^{(1)\uparrow}_{2\to 1}|\downarrow,\uparrow\rangle \Big], \end{aligned} \tag{S33}$$

$$\begin{aligned} S_{12}^{(2)\mathrm{dir}} =& - e^2\Gamma_{2e}\frac{|T_\uparrow|^2 + |T_\downarrow|^2}{\hbar^2 v_F^2} \\ &\times \sum_s \Big[||U^{(1)s}_{2\to 1}|\uparrow,\downarrow\rangle||^2 + ||U^{(1)s}_{1\to 2}|\uparrow,\downarrow\rangle||^2\Big], \end{aligned} \tag{S34}$$

$$\begin{aligned} S_1^{(2)\mathrm{exc}} =& -e\Gamma_{2e}\frac{\mathrm{Re}(T_\uparrow^\star T_\downarrow e^{i(k_\uparrow - k_\downarrow)(x_1-x_2)+i\varphi})}{\hbar^2 v_F^2} \\ &\times \Big[\langle\uparrow,\downarrow|\, U^{(1)\uparrow\dagger}_{1\to 2} U^{(1)\downarrow}_{1\to 2}|\downarrow,\uparrow\rangle + \langle\uparrow,\downarrow|\, U^{(1)\downarrow\dagger}_{2\to 1} U^{(1)\uparrow}_{2\to 1}|\downarrow,\uparrow\rangle \Big], \end{aligned} \tag{S35}$$

where $U^{(1)s}_{j\to k} = -i\int_{t_0}^\infty dt'\; \mathcal{H}^T(t')|^s_{j\to k}$ and the amplitudes are

$$\begin{aligned} \langle\uparrow,\downarrow|\mathrm{T}_{\mathcal{C}}\mathcal{H}^{Ts}_{1\to 2}(t')\mathcal{H}^{Ts}_{2\to 1}(t'')\,|\nu_1\uparrow,\nu_2\downarrow\rangle =& \frac{1}{4(2\pi)^2}\Big[f_\rho^{-1}f_\sigma^{-1}\Big](0,t';0,t'') \\ &\times \Xi_\uparrow(x_1,t_0^-;0,t'')\Xi_\uparrow(x_1,t_0^+;0,t')\Xi_\uparrow^{-1}(x_1,t_0^-;0,t')\Xi_\uparrow^{-1}(x_1,t_0^+;0,t'') \\ &\times \Xi_\downarrow(x_2,t_0^-;0,t')\Xi_\downarrow(x_2,t_0^+;0,t'')\Xi_\downarrow^{-1}(x_2,t_0^-;0,t'')\Xi_\downarrow^{-1}(x_2,t_0^+;0,t') \end{aligned} \tag{S36}$$

and

$$\begin{aligned} \langle\uparrow,\downarrow|\mathrm{T}_{\mathcal{C}}\mathcal{H}^{T\downarrow}_{1\to 2}(t')\mathcal{H}^{T\uparrow}_{2\to 1}(t'')\,|\downarrow,\uparrow\rangle =& -\frac{a^2}{4(2\pi)^2}\Big[f_\rho^{-1}f_\sigma\Big](0,t';0,t'') \\ &\times \Xi_\uparrow(x_1,t_0^-;0,t'')\Xi_\uparrow(x_1,t_0^+;0,t')\Xi_\uparrow(x_2,t_0^-;0,t'')\Xi_\uparrow(x_2,t_0^+;0,t'') \\ &\times \Xi_\downarrow^{-1}(x_1,t_0^-;0,t')\Xi_\downarrow^{-1}(x_1,t_0^+;0,t'')\Xi_\downarrow^{-1}(x_2,t_0^-;0,t'')\Xi_\downarrow^{-1}(x_2,t_0^+;0,t'). \end{aligned} \tag{S37}$$

with

$$\Xi_s = f_\rho^{-\frac{1}{2}} f_\sigma^{-\frac{s}{2}} \tag{S38}$$

Up to quantitative corrections due to modified exponents we thus recover exactly the same behavior as in the nanowire case except that in the absence of backscattering, there are as many tunneling events which decrease the current after the junction as those which increase the current. So the direct contribution is zero up to the additional features which are induced by spin-charge separation as discussed in the nanowire case. Because the Fermi vectors for spin-up and spin-down are different, the exchange current acquires an oscillating prefactor. This is essentially the same mechanism as the one induced by the Rashba effect in nanowires, and likewise introduces an additional tunable parameter.

[S1] J. von Delft and H. Schoeller, Ann. Phys. (Berlin) **7**, 225 (1998).
[S2] F. Dolcini, B. Trauzettel, I. Safi, and H. Grabert, Phys. Rev. B **71**, 165309 (2005).
[S3] A. V. Lebedev, A. Crépieux, and T. Martin, Phys. Rev. B **71**, 075416 (2005).
[S4] P. Recher, N. Y. Kim, and Y. Yamamoto, Phys. Rev. B **74**, 235438 (2006).
[S5] T. Giamarchi, *Quantum Physics in One Dimension* (Oxford University Press, 2003).
[S6] C. Wahl, J. Rech, T. Jonckheere, and T. Martin, Phys. Rev. Lett. **112**, 046802 (2014).
[S7] G. D. Mahan, *Many-Particle Physics* (Kluwer Academic/Plenum Publishers, New York, 1981).
[S8] A. Crépieux, R. Guyon, P. Devillard, and T. Martin, Phys. Rev. B **67**, 205408 (2003).
[S9] Y. Ji, Y. Chung, D. Sprinzak, M. Heiblum, D. Mahalu, and H. Shtrikman, Nature (London) **422**, 415 (2003).
[S10] I. Neder, M. Heiblum, Y. Levinson, D. Mahalu, and V. Umansky, Phys. Rev. Lett. **96**, 016804 (2006).
[S11] I. Neder, N. Ofek, Y. Chung, M. Heiblum, D. Mahalu, and V. Umansky, Nature (London) **448**, 333 (2007).
[S12] E. Bocquillon, V. Freulon, J.-M. Berroir, P. Degiovanni, B. Plaçais, A. Cavanna, Y. Jin, and G. Fève, Science **339**, 1054 (2013).
[S13] N. Ubbelohde, F. Hohls, V. Kashcheyevs, T. Wagner, L. Fricke, B. Kästner, K. Pierz, H. W. Schumacher, and R. J. Haug, Nat. Nanotechnol., advance online publication (2014), arXiv:1404.0030.
[S14] B. Karmakar, D. Venturelli, L. Chirolli, F. Taddei, V. Giovannetti, R. Fazio, S. Roddaro, G. Biasiol, L. Sorba, V. Pellegrini, and F. Beltram, Phys. Rev. Lett. **107**, 236804 (2011).
[S15] E. Bocquillon, V. Freulon, J.-M. Berroir, P. Degiovanni, B. Plaçais, A. Cavanna, Y. Jin, and G. Fève, Nat. Commun. **4**, 1839 (2013).